Talanta 81 (2010) 1760–1765

Contents lists available at ScienceDirect

Talanta

journal homepage: www.elsevier.com/locate/talanta

Electrochemical identification of corrosion products on historical and archaeological bronzes using the voltammetry of micro-particles attached to a carbon paste electrode

D. Šatović[a], S. Martinez[b,*], A. Bobrowski[c]

[a] Department of Conservation and Restoration, Academy of Fine Arts, Ilica 85, 10000 Zagreb, Croatia
[b] Department of Electrochemistry, Faculty of Chemical Engineering and Technology, Savska cesta 16, 10000 Zagreb, Croatia
[c] Faculty of Materials Science and Ceramics, University of Science and Technology, al. Mickiewicza 30, 30-059 Krakow, Poland

ARTICLE INFO

Article history:
Received 16 February 2010
Received in revised form 16 March 2010
Accepted 18 March 2010
Available online 25 March 2010

Keywords:
Voltammetry of microparticles
Bronze
Patina
Conservation and restoration
ATR-FTIR

ABSTRACT

An overview of the electrochemical method for the identification of microsampled corrosion products from historical and archaeological bronzes is reported. Two characteristic examples of long-term air and subterranean formed patinas and two artificial patinas formed on Cu-6%Sn bronze in sulphate and chloride solutions, were investigated in 0.1 M HCl(aq) by means of the cyclic voltammetry of microparticles attached to a carbon paste electrode.

Patina constituent phases were identified by comparing the electrochemical parameters of the patina samples to those of reference compounds: CuO, Cu_2O, SnO, SnO_2, CuCl, $CuCl_2 \times 2H_2O$ and $CuSO_4 \times 5H_2O$. An identification scheme was suggested which may be applied to discern the various corrosion products of bronze based on electrochemical data (voltammetric peak potentials). The presence of two prevalent phases of sulphate and chloride patinas, $CuSO_4$ and CuCl, as well as the presence of Sn compounds was clearly indicated by the cyclic voltammetry of microparticles, in both, naturally and artificially formed samples. A comparison to the ATR-FTIR results revealed that the methods are complementary and that their simultaneous application could prove particularly valuable in drawing conclusions about the current shape and prospects of the conservation and restoration of bronze artefacts.

1. Introduction

The deterioration of historical and archaeological bronze artefacts is mostly caused by electrochemical corrosion [1]. Ancient bronzes are usually very heterogeneous, and thus corrode easily forming various corrosion product surface layers (patinas) [2,3]. Knowledge on patina constituent phases and the mechanisms of their formation plays an essential role in understanding the deterioration of bronze artefacts. This knowledge may also help in predicting the corrosion behaviour of bronze under different environmental conditions (i.e. after excavation or a change in storage climate in museums) and in devising conservation-restoration measures that are needed to protect bronze from further deterioration. It has been shown that the use of electrochemical methods is particularly prospective for both purposes [4–8]. Various types of electrochemical measurements of bronze corrosion products removed from archaeological artefacts were presented in a few other papers published on this subject matter [9–11].

The aim of the present study was to investigate how the electrochemical method of the voltammetry of microparticles (VMP) on a carbon paste electrode (CPE) can be used to perform an electrochemical identification of bronze patinas.

Scholz and co-workers introduced the VMP method to analytical practice in 1998 as a new tool in electrochemical analysis. Initially called Abrasive Stripping Voltammetry [12], VMP quickly found its application in the investigation of electrochemical and surface properties of a great variety of solid materials. A theoretical model explaining electron transfer processes involving nonconducting solid microparticles, applicable to the results of the present study [13], was developed by Lovric and Scholz [14,15] and Oldham [16]. Of significant importance is the fact that the solid-state processes in microparticles are phase-characteristic, which enables the electrochemical identification of the respective solid materials, and the acquisition of valuable information about their redox state and physical phases [9,17].

In the present paper, VMP was applied to a carbon paste electrode (CPE) for electrochemical identification and the characterization of corrosion products collected from two bronze artefacts with naturally formed (atmospheric and subterranean) patinas and two bronze (Cu-6%Sn) sheets with patinas artificially formed through immersion in the electrolyte. One of the investigated, nat-

* Corresponding author. Tel.: +385 1 4597116; fax: +385 1 4597139.
E-mail addresses: dsatovic@alu.hr (D. Šatović), sanja.martinez@fkit.hr (S. Martinez), abobrow@agh.edu.pl (A. Bobrowski).

0039-9140/$ – see front matter © 2010 Elsevier B.V. All rights reserved.
doi:10.1016/j.talanta.2010.03.037

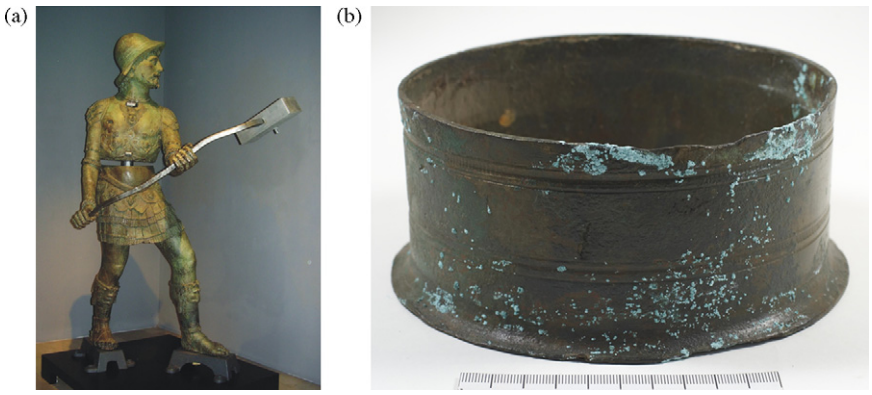

Fig. 1. a) Renaissance bronze sculptures Maro and Baro from the town belfry of Dubrovnik and b) archaeological bronze "Roman wheel" from the 1st century A.D. used for collecting naturally formed patina samples.

urally formed patinas, originated from the Zelenci Renaissance sculptures: Maro and Baro from the town belfry of Dubrovnik, dating from 1478. Zelenci, or "Jacquemarts", as art historians often call these types of sculptures are two bronze statues of men, clad in Roman armour, striking the hours. These sculptures are the only two bronze sculptures from that period in Croatia. They were probably made by Michelozzo di Bartolomeo (1391-1472), a famous Renaissance architect and sculptor from Tuscany. He was invited by the Ragusan government and spent four years from 1461 to 1464 in the city of Dubrovnik working on the extension of the city walls and the city tower [18]. Maro and Baro were exposed to marine air during their functional use on the town belfry of Dubrovnik until they were replaced with replicas in 2003. Samples were collected from the left leg of one of the original "Jacquemarts" (Fig. 1a). The second naturally formed patina that was investigated originated from the bronze part of a „Roman wheel" found near Zagreb, dating from the 1st century A.D. (Fig. 1b).

2. Experimental

The reference materials used were commercial p.p.a. chemicals (P.P.H. Polskie Odczynniki Chemiczne Gliwice): CuO, Cu_2O, $CuSO_4$, SnO, SnO_2, CuCl and $CuCl_2 \times 2\ H_2O$. Approximately 10-20 μg of these compounds were powdered in a mortar and spread on a fine paper sheet, forming a thin layer of finely distributed micro-particles. The micro-particles were attached to the surface of the CPE by gently rubbing the layer. The electrode was then rinsed with distilled water to remove any loosely attached particles. Carbon paste was prepared from graphite powder (Fluka, puriss< 20 μm) and paraffin oil (Merck) mixed in a 5:1 ratio and thoroughly homogenised using a pestle and mortar. A special piston-driven electrode holder was filled with the paste using a spatula. This specially designed electrode holder allows a very precise extraction of carbon paste by the screw positioned at the top of the electrode. The details of the electrode construction have been provided by Lu et al. [19]. The electrode surface was renewed after every scan by rubbing the electrode surface on wet filter paper and then polished on a glass surface. The exposed surface of the electrode was circular and 0.3 cm in diameter.

Cyclic voltammetry measurements were carried out in a conventional three electrode electrochemical cell consisting of a carbon paste electrode, Hg/HgCl/KCl (sat.), and a platinum wire as the working, reference, and counter electrode, respectively. A μAUTOLAB device (Eco Chemie B.V., Utrecht, The Netherlands), controlled using GPES software (Eco Chemie B.V., Utrecht, The Netherlands, Version 4.9), was employed in the measurements. The electrolyte, 0.1 M HCl(aq), was degassed with Argon gas for 5 minutes prior to the measurements. All measurements were carried out at room temperature.

Voltammetric cycles were measured, at a scan rate of 30 mVs^{-1}, in the potential range between -1.2 and +1.2 V starting from the open circuit potential (E_{OC}) in the following directions: (i) anodic and (ii) cathodic.

A new sample of the material attached to the surface of the carbon paste electrode was used in each measurement. Three voltammetric cycles were performed for each sample.

Cu-6%Sn bronze coupons were used to produce corrosion layers, which were later analysed using VMP and ATR/FTIR. The formation of artificial patinas on bronze coupons was done by immersion for a period of 6 days in solutions simulating atmospheric urban acid and marine environments, respectively as follows: 0.2 g/l Na_2SO_4 + 0.2 g/l $NaHCO_3$ (acidified to pH = 5 with diluted H_2SO_4), and 0.7 g/l NaCl. Prior to immersion, the coupons were mechanically treated with P 800 abrasive paper, then P 1200, degreased with ethanol, immersed in 10% (wt) H_2SO_4 for 1 minute and finally air-dried at room temperature. All corrosion layer formation experiments were carried out in a 1 dm^3 laboratory vessel, at room temperature (25 ± 1 C°). The volume-to-surface specimen area was 20 mL × cm^{-2} according to the ASTM G 31 (1990) standard [20]. Examinations of the surface morphology of the samples were carried out using a Philips XL 30 scanning electron microscope. The elemental composition of the corrosion product layers formed on the surface, was determined using quantitative energy dispersive X-ray spectroscopy (EDX) attached to the SEM. An attenuated total reflectance Fourier transform infrared spectroscopy (ATR FTIR) was carried out using a Bruker Vertex 70 FTIR spectrometer. Spectra were collected at a resolution of 4 cm^{-1}, between 400 and 4000 cm^{-1}.

3. Results and discussion

3.1. Voltammetry of reference materials

The representative voltammograms that measured for reference materials by means of VMP in 0.1 M HCl(aq) (pH = 1.0) are presented in Figs. 2 and 3. The voltammetric peaks of the investigated samples are presented in Table 1. Additionally, E_{OC} that represents the starting point of the measurements is also given in Table 1.

The voltammetric cycles of reference compounds started at E_{OC} in the anodic direction are shown partially (from E_{OC} to + 1.2 V and back to E_{OC}) in Fig. 3. Anodic peaks were observed only for low valence Cu and Sn reference compounds, i.e. at 0.507 ± 0.042 V for Cu_2O and CuCl and at −0.387 ± 0.021 for SnO. These anodic peaks correspond to the oxidation of Cu(I) to Cu(II) and Sn(II) to Sn(IV).

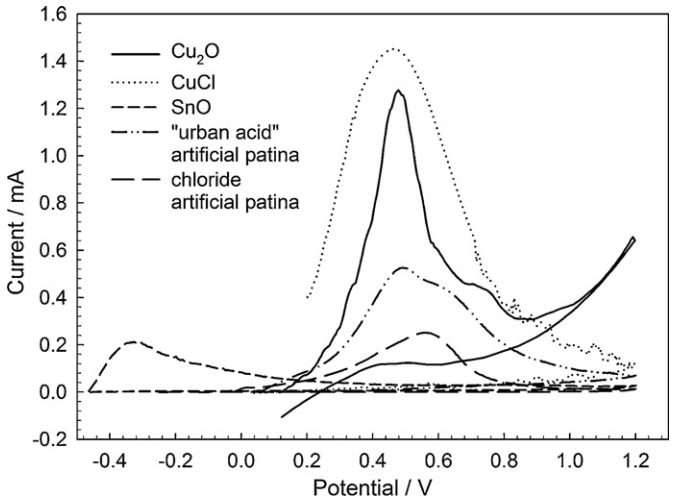

Fig. 2. Anodic parts of cyclic voltammograms recorded in 0.1 M HCl for selected reference compounds and artificially formed patinas measured by starting at E_{OC} in the cathodic direction. Scan rate was set at 30 mVs^{-1}.

The voltammetric cycles of reference compounds started at E_{OC} in the cathodic direction are shown in full in Fig. 3. When the scan preformed from E_{OC} to -1.2 V and back to E_{OC} is continued into the anodic region, all the reference compounds show multiple anodic peaks. The anodic peaks obtained after the cathodic scan were not analysed further, as they were very poorly defined due to their overlap, and did not reflect the native state of the samples.

In the cathodic scan, from E_{OC} to - 1.2 V and back to E_{OC}, the cathodic peaks were observed for all patinas and reference compounds with the exception of SnO_2. In general, the peaks appeared in three potential regions: region I–from +0.2 to–0.3 V, region II–from -0.3 to -0.7 V and region III–from −0.7 to −1.2 V.

The proposed electrochemical reduction reactions of the copper reference compounds that occur in the cathodic scan may be written as follows [9,21,22]:

$$CuO_{(s)} + 2H^+ + 2e^- \rightarrow Cu_{(s)} + H_2O \quad (1)$$

$$Cu_2O_{(s)} + 2H^+ + 2e^- \rightleftarrows 2Cu_{(s)} + H_2O \quad (2)$$

$$CuCl_{(s)} + e^- \rightleftarrows Cu_{(s)} + Cl^- \quad (3a)$$

$$CuCl_{2(s)} + e^- \rightleftarrows CuCl_{(s)} + Cl^- \quad (3b)$$

$$CuCl_{2(s)} + e^- \rightleftarrows Cu^{2+}_{(aq)} + 2Cl^- + 2e^- \rightleftarrows Cu_{(s)} \quad (4)$$

$$CuSO_{4(s)} \rightleftarrows Cu^{2+}_{(aq)} + SO^{2-}_4 + 2e^- \rightleftarrows Cu_{(s)} \quad (5)$$

The solid state reduction processes of copper oxides and chlorides are complex, since their progress requires protons to penetrate the lattice and proton and/or electron hopping through the lattice, finally leading to a solid state reaction yielding $Cu_{(s)}$ as the new solid phase [9]. Consequently, the reduction process is initiated at the three-phase electrode surface/particle/supporting electrolyte boundary and is restricted to a relatively narrow region in the lateral faces of the crystals. Additionally, the reductive dissolution of copper on the surface of the particles is followed by the electrodeposition step, making the overall process dependent on the kinetics of copper nucleation and nucleus growth.

The solubility of the compounds also appears to influence the reduction reactions. The intensities of the cathodic peak currents are lower by one order of magnitude for $CuSO_4$ (peak current ~ 0.1 mA) and by two orders of magnitude for $CuCl_2$ (peak current ~ 0.01 mA) than for other reference compounds containing copper (peak current ~ 1 mA), indicating a loss of electrode material through chemical dissolution. This assumption is substantiated by the fact that in subsequent cycles both the oxidation and reduction peaks of $CuSO_4$ and $CuCl_2$ diminish rapidly (not shown), which indicates the occurrence of a fast chemical dissolution [23]. The influence of chemical dissolution was therefore assumed for $CuSO_4$ and $CuCl_2$ and is expressed in equations 4 and 5.

In region III of Fig. 3a, cathodic peaks were exhibited by CuO, Cu_2O and CuCl. The voltammetric response in this range of potentials corresponds to the reduction of microcrystals to metallic copper. The negativity of the peak potential probably originates from the "break-in" overpotential related to the energy required to destroy the crystal structure of the particle [24].

In region II of Fig. 3a, Cu_2O and CuCl showed cathodic peaks corresponding to the Cu(I) → Cu(0) solid state transition trough reactions 2 and 3a.

As expected, the mixture of CuO and Cu_2O exhibited peaks in potential regions, I and II. Poor peak resolution arises as a consequence of the superposition of signals for constituent phases that contribute to the complex mixture to a different extent.

In region II of Fig. 3b, the peaks observed for $CuCl_2$ and $CuSO_4$ are probably due to the reduction of Cu^{2+} originating from the preceding chemical dissolution reactions (4 and 5).

In region I of Fig. 3a and b, the observed cathodic peaks belonged to CuCl and $CuCl_2$ (Fig. 3 b and c, Table 1) and were probably due to the solid-state one-electron reduction process of Cu(II) to Cu(I) (equation 3b). Since it is known that CuCl patina is easily oxidized in moist air, the appearance of this peak for CuCl may could be explained by the occurrence of the chemical oxidation of CuCl in air during the period of storage and/or attachment to the electrode [25].

Table 1
Electrochemical parameters of representative VMP measurements for reference compounds and patinas.

Compound	E_{OC} /V	Anodic peak /V	Cathodic peak in region I /V	Cathodic peak in region II /V	Cathodic peak in region III /V
Cu species					
Cu_2O	+ 0.080	+0.468	-	-0.561	-
CuO	+ 0.400	-	-	-	-0.973
CuCl	+0.256	+0.461	-0.134	-0.639	< -0.7
$CuCl_2$	+0.285	-	+0.060	-0.370	-
$CuSO_4$	+0.350	-	-	-0.305	-
Cu_2O, CuO mixture	+0.108	+0.588	-	unresolved	-0.927
Sn species					
SnO	-0.465	-0.329	-	-	-0.605; -0.820; -0.940
SnO_2	+0.142	-	-	-	-
Patinas					
Roman wheel patina	+0.355	-	-0.105	-0.365	-0.605; -0.825; -0.945
"Jacquemarts" patina	+0.299	-	-	-0.301	-
chloride artificial patina	-0.060	+0.556	-0.146	-0.241	-
"urban acid" artificial patina	-0.029	+0.490	-	-0.284	-

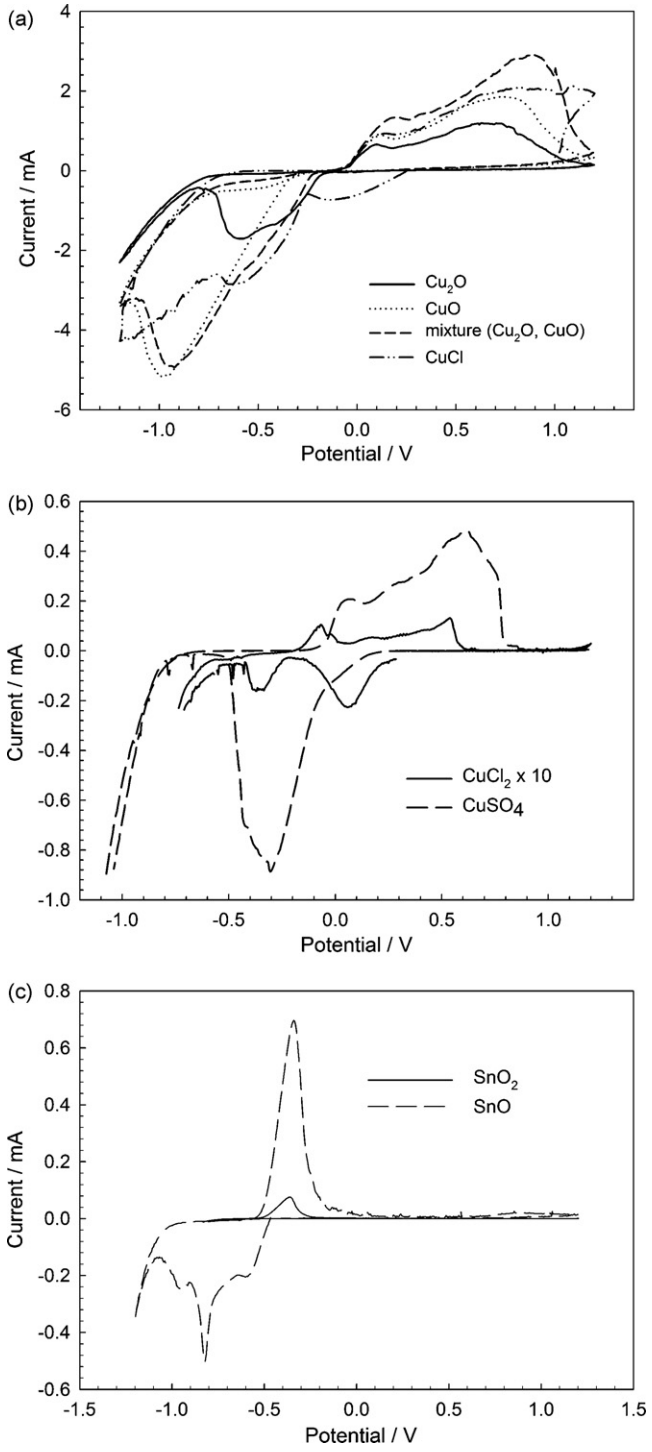

Fig. 3. Cyclic voltammograms recorded in 0.1 M HCl for all reference compounds measured by starting at E_{OC} in the cathodic direction. Scan rate was set at 30 mVs^{-1}.

It is noteworthy that the assumed Cu(II) → Cu(0) reduction occurs at potentials approx. 0.2 V more negative than the Cu(II) → Cu(I) solid state transition, and by approx. 0.25 V more positive than the Cu(I) → Cu(0) solid state transition.

SnO_2 did not show any cathodic peaks (Fig. 3c). Only after the initial cathodic scan to -1.2 V did the anodic peak at -0.387 ± 0.021 V appear, upon polarization to potentials more positive than E_{OC} (Fig. 3c). As in the case of SnO, this peak corresponds to the Sn(II) → Sn(IV) transition. This voltammetric response can be explained by the stability of SnO_2 in chloride media.

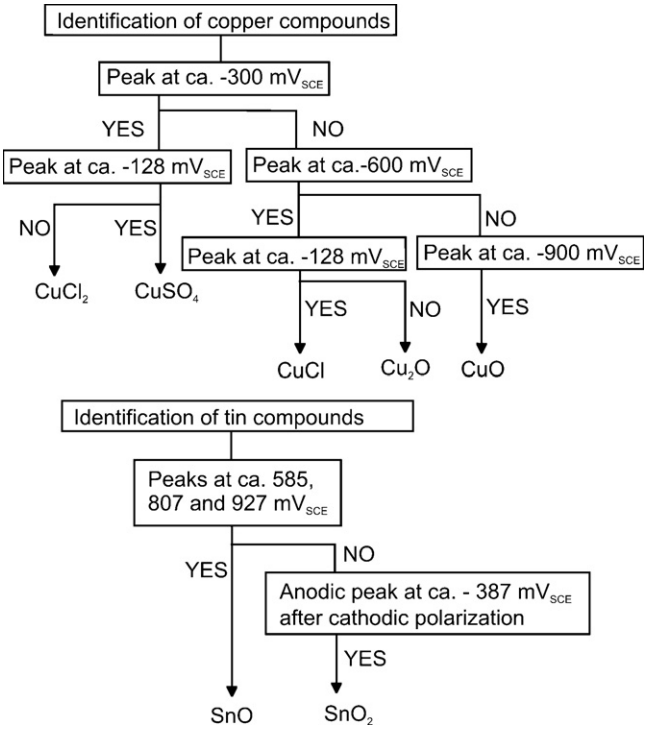

Fig. 4. An identification scheme which may be applied to discern between the various corrosion products of bronze based on VMP electrochemical data. Scan rate was set at 30 mVs^{-1}.

SnO, on the other hand, showed one sharp cathodic peak at -0.807 ± 0.017 V in the negative scan with shoulders at 0.585 ± 0.010 and -0.927 ± 0.017 V, which indicates that the reduction of SnO is a stepwise process that probably reflects the complexation of the Sn species with chloride ions.

An identification scheme which may be used to discern the various corrosion products of bronze based on voltammetric data is presented in Fig. 4.

3.2. Voltammetry of patinas

It is known that the patinas on historical bronzes are complex mixtures of various copper and tin compounds [26]. Their voltammograms were therefore compared to the voltammograms of the reference materials. The electrochemical parameters deduced from the representative cyclic voltammograms of patina samples are provided in Table 1. The voltammetric cycles of patinas started at E_{OC} in the anodic direction are shown partially (from E_{OC} to + 1.2 V and back to E_{OC}) in Fig. 3. The anodic peaks were observed only for the artificial patinas indicating the presence of low valence copper compounds.

Cyclic voltammograms of patina samples started in the cathodic direction are shown in full in Fig. 5a and b. The scan for the „Jacquemarts" patina (Fig. 5a) revealed a single cathodic peak implying the presence of $CuSO_4$. The multiple peaks that appeared in the voltammogram of the „Roman wheel" (Fig. 5a) patina unequivocally indicated the presence of both $CuCl_2$ and SnO. Due to the positivity of E_{OC} that approaches that of the copper constituent compounds, the anodic peak of SnO was recorded only after the cathodic scan had been conducted. (Fig. 5a)

In order to confirm the presence of tin in the „Jacquemarts" patina and its absence in the „Roman wheel" patina, an EDX analysis was conducted. Table 2 summarizes the average content of elements present in the analyzed samples, expressed as mass and atomic percentage. The patinas of both samples consist mostly

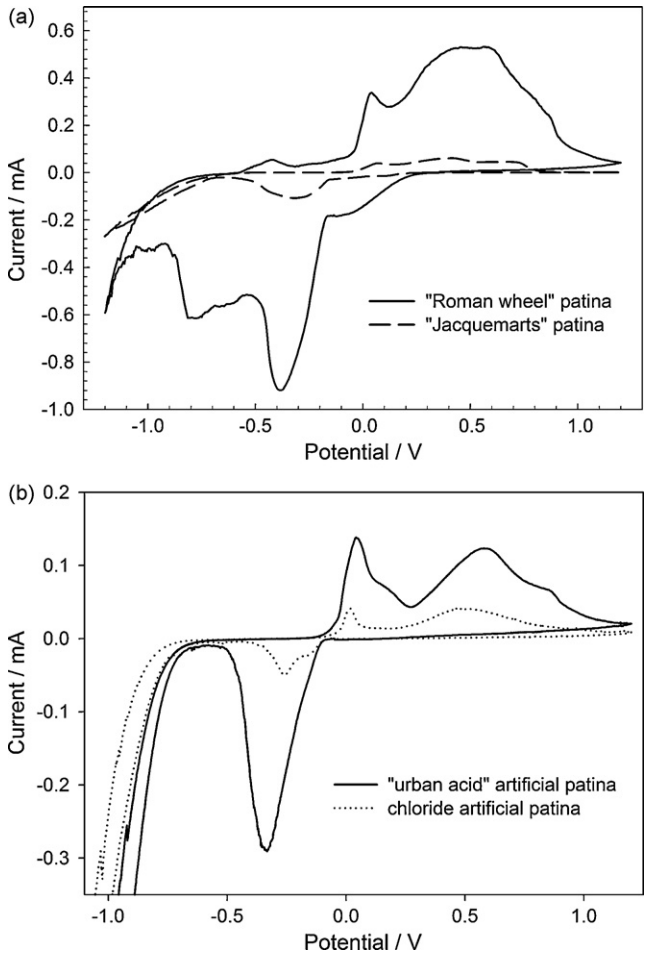

Fig. 5. Cyclic voltammograms recorded in 0.1 M HCl for all a) naturally formed and b) artificially formed patinas, measured by starting at E_{OC} in the cathodic direction. Scan rate was set at 30 mVs^{-1}.

of oxygen, carbon and copper, with some sulphur content. There were considerable amounts of chlorine and tin in the „Roman wheel" patina sample, while the „Jacquemarts" patina contained a significant amount of sulphur, which was consistent with the voltammetric results.

3.3. ATR-FTIR analysis of patinas

The ATR-FTIR spectra of patina samples are shown in Fig. 6. The measured spectra coincide with that of langite ($Cu_4SO_4(OH)_6 \times 2H_2O$) in the case of the „Jacquemarts" patina (Fig. 6a), and that of atacamite ($Cu_4Cl_2(OH)_6$) [27] in the case of the „Roman wheel" patina (Fig. 6b). The bands peaking at 3299 and 3436 cm^{-1} and at 979 and 931 cm^{-1} are characteristic of atacamite [28], while the typical sulphate band appears at 1050–1100 cm^{-1} [29]. These results are also consistent with the voltammetric ones, pointing to the prevalence of Cu(II)-sulphate compounds and Cu(II)-chloride compounds in the „Jacquemarts" and „Roman wheel" patinas, respectively. However, the apparent presence of SnO in the „Roman wheel" patina, as indicated by voltammetric analysis and substantiated by the EDX measurements, was not obvious from the ATR-FTIR. The absorption bands at 540 cm^{-1}, ascribed to the terminal oxygen vibration in SnOH,

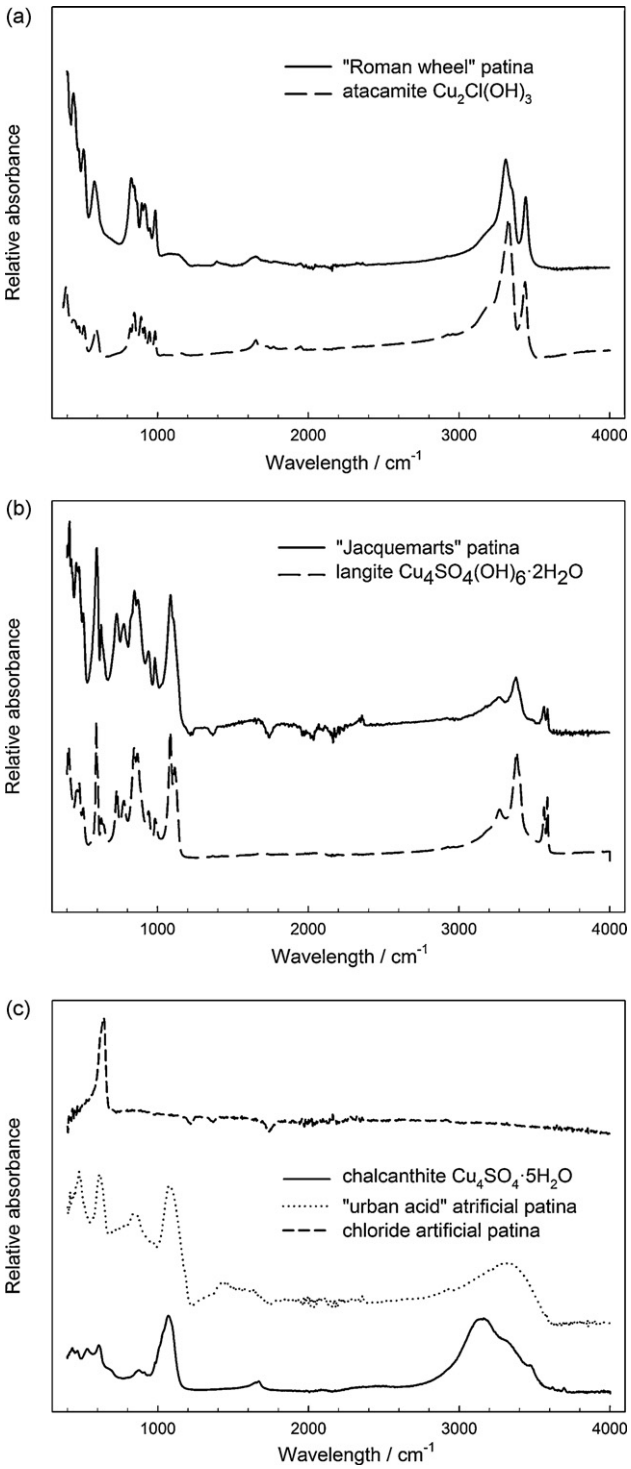

Fig. 6. ATR-FTIR results for: the naturally formed a) "Roman wheel" and b) "Jacquemarts" patinas and c) artificially formed patinas, compared to the ATR-FTIR spectra of reference compounds.

Table 2
EDX results of the weight (wt%) and atomic (at%) ratio of the elements present in the patinas.

Element	„Roman wheel" patina		„Jacquemarts" patina	
	Wt %	At %	Wt %	At %
O (K)	42.25	59.90	64.75	78.10
Cu (K)	19.60	7.00	19.86	6.03
Cl (K)	15.32	9.80	/	/
C (K)	10.63	20.08	6.57	10.55
Sn (L)	6.40	1.22	/	/
Sb (L)	4.01	0.75	/	/
S (K)	1.78	1.26	8.82	5.31

and at 480 cm^{-1} and 630 cm^{-1}, ascribed to the stretching frequencies of oxide groups in SnO and SnO_2, respectively, were not recorded [30,11]. Furthermore, the bands at 1419 and 873 cm^{-1} corresponding to carbonate stretching modes were not visible in either spectrum [31]. On the other hand, the presence of OH functions was indicated only by the ATR-FTIR results (hydroxyl groups located in the 3300-3600 cm^{-1} region for both patinas, and water at 1633 cm^{-1} in the case of the „Roman wheel" patina) [29].

The ATR-FTIR spectrum (Fig. 6c) of the chloride artificial patina showed a single band corresponding to Cu_2O at 646 cm^{-1} [11]. Similarly, Cu_2O is also indicated in the ATR-FTIR spectrum of the "urban acid" artificial patina as a prominent band at 625 cm^{-1} (Fig. 6c). This is consistent with the appearance of anodic oxidation peaks in Fig. 2.

Additionally, the "urban acid" artificial patina shows a band at 487 cm^{-1} that can originate from stretching the oxide group in SnO. The rest of the ATR-FTIR spectrum closely resembles that of chalcanthite ($CuSO_4{\cdot}5H_2O$), also showing a typical sulphate band [29]. Sn species were not observed in the voltammogram of the "urban acid" patina, but the presence of sulphates is clearly indicated by the cathodic peak at −0.284 V in Fig. 5b.

4. Conclusions

The cyclic voltammetry of the microparticles of bronze corrosion product compounds attached to a carbon paste electrode provided well-defined electrochemical responses characteristic of various Cu and Sn compounds. The recognition of the constituent phases was based on the association of the voltammetric peaks for the reference materials and those obtained for the patina samples in the first voltammetric runs measured from E_{OC} to +1.2 V or -1.2 V. The results made it possible to clearly differentiate between the natural and the artificial chloride/sulphate patinas, while at the same time yielding valuable information about the redox state of the samples.

A comparison of the cyclic voltammetry of microparticles and ATR-FTIR methods has shown that these methods complement one another. Given the information deduced from the combined results, it is reasonable to assume that the simultaneous application of both methods could prove particularly valuable in drawing conclusions about the current shape and prospects of the conservation and restoration of bronze artefacts.

References

[1] J.H. Payer, Bronze corrosion: rates and chemical processes, in: T. Drayman-Weisser (Ed.), Dialogue/89, The Conservation of Bronze Sculpture in the Outdoor Environment: A Dialogue Among Conservators, Curators, Environmental Scientists, and Corrosion Engineers, NACE Houston, 1992, pp. 103–121.

[2] C. Chiavari, K. Rahmouni, H. Takenouti, S. Joiret, P. Vermaut, L. Robbiola, Composition and electrochemical properties of natural patinas of outdoor bronze monuments, Electrochim. Acta 52 (2007) 7760–7769.

[3] L. Robbiola, J. Blengino, C. Fiaud, Morphology and mechanism of formation of natural patinas of archaeological Cu–Sn alloys, Corr. Sci. 40 (1998) 2083–2111.

[4] H. Hassairi, L. Bousselmi, E. Triki, Bronze degradation processes in simulating archaeological soil media, J. Solid State Electrochem. 14 (2010) 393–401.

[5] D. Šatovic, L. Valek Žulj, V. Desnica, S. Fazinić, S. Martinez, Corrosion evaluation and surface characterization of the corrosion product layer formed on Cu–6Sn bronze in aqueous Na_2SO_4 solution, Corr. Sci. 51 (2009) 1596–1603.

[6] F. Rodríguez-Acuña, J. Genescá, J. Uruchurtu, Electrochemical evaluation of patinas formed on nineteenth century bronze bells, J. Appl. Electrochem. 40 (2010) 311–320.

[7] A. Adriaens, M. Dowsett, In-situ spectroelectrochemical studies of the removal of chlorides from copper, Metal07 3 (2007) 10–14.

[8] E. Rocca, F. Mirambet, The electrochemical techniques for the diagnosis and restoration treatments of technical and industrial heritage: three examples of metallic artefacts, J. Solid State Electrochem. 14 (2010) 415–423.

[9] A. Domenech-Carbo, M.T. Domenech-Carbo, I. Martinez-Lazaro, Electrochemical identification of bronze corrosion products in archaeological artefacts. A case study, Microchim. Acta 162 (2008) 351–359.

[10] N. Souissi, L. Bousselmi, S. Khosrof, E. Triki, Voltammetric behaviour of an archaeological bronze alloy in aqueous chloride media, Materials and Corrosion 55 (2004) 284–292.

[11] M. Serghini-Idrissi, M.C. Bernard, F.Z. Harrif, S. Joiret, K. Rahmouni, A. Srhiri, H. Takenouti, V. Vivier, M. Ziani, Electrochemical and spectroscopic characterizations of patinas formed on an archaeological bronze coin, Electrochim. Acta 50 (2005) 4699–4709.

[12] F. Scholz, B. Meyer, Voltammetry of solid microparticles immobilized on electrode surfaces, in: A.J. Bard, I. Rubinstein (Eds.), Electroanalytical Chemistry, vol. 20, Marcel Dekker, New York, 1998, pp. 1–86.

[13] A. Domenech-Carbo, M.T. Domenech-Carbo, V. Costa, Electrochemical Methods in Archaeometry, Conservation and Restoration, Springer-Verlag, Heidelberg, 2009, pp. 33–55.

[14] M. Lovric, F. Scholz, A model for the propagation of a redox reaction through microcrystals, J. Solid State Electrochem. 1 (1997) 108–113.

[15] M. Lovric, F. Scholz, A model for the coupled transport of ions and electrons in redox conductive microcrystals, J. Solid State Electrochem. 3 (1999) 172–175.

[16] K.B. Oldham, Voltammetry at a three-phase junction, J. Solid State Electrochem. 2 (1998) 367–377.

[17] G. Cepriá, A. Usón, J. Pérez-Arantegui, J.R. Castillo, Identification of iron(III) oxides and hydroxy-oxides by voltammetry of immobilised microparticles, Anal. Chim. Acta 477 (2003) 157–168.

[18] I. Fisković, Dubrovački "Zelenci", Prilozi povijesti umjetnosti u Dalmaciji 31 (1991) 151–176.

[19] Z.Y. Lu, M.I. Jeffrey, F. Lawson, An electrochemical study of the effect of chloride ions on the dissolution of chalcopyrite in acidic solutions, Hydrometallurgy 56 (2000) 145–155.

[20] ASTM G 31-72 Standard practice for laboratory immersion corrosion testing of metals, ASTM, 1990, 102–108.

[21] A.B.A. Sedano, M.L. Tascon Garcıa, M.D. Vazquez Barbado, P.S. Batanero, Electrochemical study of copper and iron compounds in the solid state by using voltammetry of immobilized microparticles: application to copper ferrite characterization, J. Electroanal. Chem. 566 (2004) 433–441.

[22] Š. Komorsky-Lovrić, Lj. Marinić-Pajc, N. Tadej, A.J.M. Horvat, J. Petran, Voltammetry of copper oxide micro-particles immobilised on diatomite surface, J. Electroanal. Chem. 623 (2008) 75–80.

[23] Š. Komorsky-Lovrić, A.J.M. Horvat, D. Ivanković, Characterization of Bronzes by Abrasive Stripping Voltammetry and Thin Layer Chromatography, Croat. Chem. Acta. 79 (2006) 33–39.

[24] P. Piccardo, B. Mille, L. Robbiola, Tin and copper oxides in corroded archaeological bronzes, in: P. Dillman, G. Beranger, P. Piccardo, H. Matthiesen (Eds.), Corrosion of Metallic Heritage Artefacts, Woodhead Publishing Limited, Cambridge, 2007, pp. 239–260.

[25] R.T. Downs, The RRUFF Project: an integrated study of the chemistry, crystallography, Raman and infrared spectroscopy of minerals, in: Program and Abstracts of the 19th General Meeting of the International Mineralogical Association, IMA, Kobe, 2006, pp. 3–13.

[26] C. Giangrande, Identification of bronze corrosion products by infrared absorption spectroscopy, in: J. Black (Ed.), Jubilee Conservation Conference Papers: Recent advances in the conservation and analysis of artefacts, Summer School Press, University of London, 1987, pp. 135–148.

[27] E. Sidot, N. Souissi, L. Bousselmi, E. Triki, L. Robbiola, Study of the corrosion behaviour of Cu–10Sn bronze in aerated Na_2SO_4 aqueous solution, Corr. Sci. 48 (2006) 2241–2257.

[28] T. Krishnakumar, K. Nicola Pinna, K. Prasanna Kumari, R. Perumal, Jayaprakash, Microwave-assisted synthesis and characterization of tin oxide nanoparticles, Mat. Lett. 62 (2008) 3437–3440.

[29] C.E. Silva, L.P. Silva, H.G.M. Edwards, L.F.C. de Oliveira, Diffuse reflection FTIR spectral database of dyes and pigments, Anal. Bioanal. Chem. 386 (2006) 2183–2191.